AD-A125 885 A 10 CM DUAL FREQUENCY DOPPLER WEATHER RADAR PART I THE RADAR SYSTEM(U) AIR FORCE GEOPHYSICS LAB HANSCOM AFB MA A W BISHOP ET AL. 25 OCT 82 AFGL-TR-82-0321(I) 1/1

UNCLASSIFIED F/G 17/9 NL

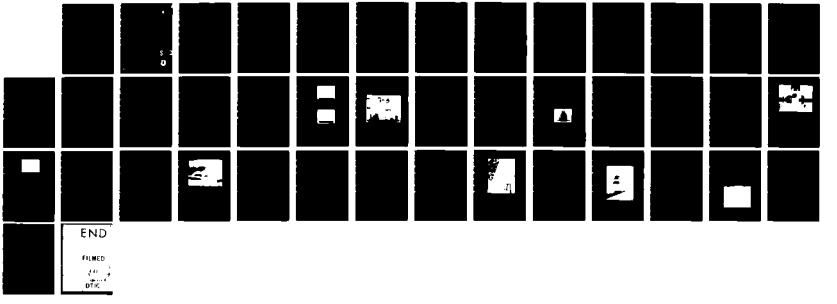

END

FILMED

DTIC

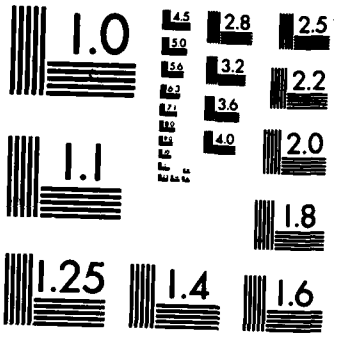

AFGL-TR-82-0321(I)
INSTRUMENTATION PAPERS, NO. 313(I)

A 10 cm Dual Frequency Doppler Weather Radar

Part I: The Radar System

ALEXANDER W. BISHOP
GRAHAM M. ARMSTRONG

25 OCTOBER 1982

METEOROLOGY DIVISION
PROJECT 6670
AIR FORCE GEOPHYSICS LABORATORY
HANSCOM AFB, MASSACHUSETTS 01731

AIR FORCE SYSTEMS COMMAND, USAF

This report has been reviewed by the ESD Public Affairs Office (PA) and is releasable to the National Technical Information Service (NTIS).

This technical report has been reviewed and is approved for publication.

Alva T Stair Jr.

DR. ALVA T. STAIR, Jr
Chief Scientist

Qualified requestors may obtain additional copies from the Defense Technical Information Center. All others should apply to the National Technical Information Service.

Unclassified

SECURITY CLASSIFICATION OF THIS PAGE (When Data Entered)

REPORT DOCUMENTATION PAGE		READ INSTRUCTIONS BEFORE COMPLETING FORM
1. REPORT NUMBER AFGL-TR-82-0321(I)	2. GOVT ACCESSION NO.	3. RECIPIENT'S CATALOG NUMBER
4. TITLE (and Subtitle) A 10 cm DUAL FREQUENCY DOPPLER WEATHER RADAR Part I: The Radar System		5. TYPE OF REPORT & PERIOD COVERED Scientific. Final. 6. PERFORMING ORG. REPORT NUMBER IP, No. 313(I)
7. AUTHOR(s) Alexander W. Bishop Graham M. Armstrong		8. CONTRACT OR GRANT NUMBER(s)
9. PERFORMING ORGANIZATION NAME AND ADDRESS Air Force Geophysics Laboratory (LYR) Hanscom AFB Massachusetts 01731		10. PROGRAM ELEMENT, PROJECT, TASK AREA & WORK UNIT NUMBERS 62101F 66700601
11. CONTROLLING OFFICE NAME AND ADDRESS Air Force Geophysics Laboratory (LYR) Hanscom AFB Massachusetts 01731		12. REPORT DATE 25 October 1982 13. NUMBER OF PAGES 42
14. MONITORING AGENCY NAME & ADDRESS(if different from Controlling Office)		15. SECURITY CLASS. (of this report) Unclassified 15a. DECLASSIFICATION DOWNGRADING SCHEDULE
16. DISTRIBUTION STATEMENT (of this Report) Approved for public release; distribution unlimited.		
17. DISTRIBUTION STATEMENT (of the abstract entered in Block 20, if different from Report)		
18. SUPPLEMENTARY NOTES		
19. KEY WORDS (Continue on reverse side if necessary and identify by block number) Doppler weather radar Dual frequency radar Diplexer Dual channel receiver Coherent frequency source Radar transmitters Power distribution Next Generation Weather Radar (NEXRAD)		
20. ABSTRACT (Continue on reverse side if necessary and identify by block number) Design concepts and test results are summarized for a Doppler weather radar system suitable for precipitation measurements over a wide span of radial velocities and slant ranges, even in the presence of ground clutter. The radar transmits two uniform pulse trains at 2.710 and 2.760 GHz. Uniformly spaced pulses permit ground clutter cancellation of up to 50 dB to be achieved with a three-pole elliptic filter. Pulse spacing at one frequency is consistent with long-range coverage in reflectivity, while spacing of the second is consistent with a wide unambiguous velocity measurement span.		

DD FORM 1 JAN 73 1473 EDITION OF 1 NOV 65 IS OBSOLETE

Unclassified

SECURITY CLASSIFICATION OF THIS PAGE (When Data Entered)

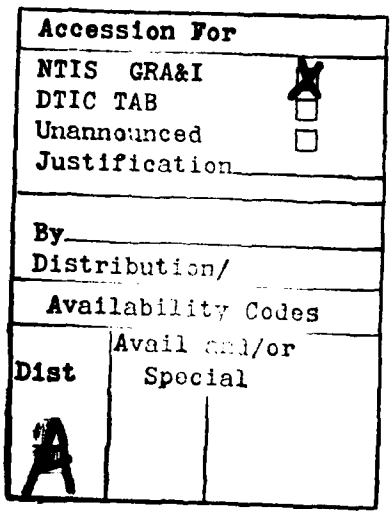

Preface

Many people contributed to the development of this radar. The authors are especially grateful to Mr. Kenneth Glover, Chief of the AFGL Ground-Based Remote Sensing Branch, for his encouragement and support throughout the project and his review and critique of the manuscript. William Smith, Edward Duquette, Ruben Novack and SSgt Charles Klein worked diligently in fabricating and testing the system. The computer-controlled receiver calibrations would not have been possible without the efforts of Capt Douglas Forsyth who wrote the software and designed the interface hardware from the computer to the receiver calibration logic. Kenneth Banis and Major Carlton Bjerkaas provided many helpful discussions during the course of the work unit. Without George Ritscher and Allen Gatinella the building and radome to house the radar would not have been realized. With all of these and many other helpful people we have failed to list, we have successfully completed the design, fabrication and testing of this dual frequency radar.

This report encompasses only the basic radar and not the system as a whole. Included as part of the system and published under separate covers are the "Quality Assurance/Fault Location Network" and "The Radar Monitor, Control and Evaluation System". The Quality Assurance/Fault Location Network makes use of fault location techniques at critical locations in the radar and quasi-continuous monitoring of radar performance. The Radar Monitor, Control and Evaluation System provides for automated system calibration and operator interactive control of the computer and data displays.

Contents

1. INTRODUCTION 9

2. SYSTEM CONFIGURATION 10

3. SYSTEM DESCRIPTION 15

3.1 Transmitter 15
3.1.1 Coherent Frequency Source 15
3.1.2 Pulse Repetition Time Generator 20
3.1.3 Transmitters 22
3.2 R. F. Transmission 24
3.2.1 Diplexer 24
3.2.2 High Power Circulator and Directional Couplers 26
3.2.3 TR Limiter 26
3.2.4 Waveguide Arc Detection 27
3.3 Receiver 28
3.3.1 Dual Frequency Receiver 28
3.3.2 Receiver Noise Figure 30
3.3.3 Calibration 31
3.3.3.1 Receiver 31
3.3.3.2 System 34
3.4 Antenna and Radome 35
3.5 Station Primary Power 39

4. CONCLUDING REMARKS 39

Illustrations

1. Transmitter Timing Sequence for the Dual Frequency Radar 12
2. Functional Block Diagram of the 10 cm Dual Frequency Doppler Radar Transmitting and Receiving Equipments 13
3. Functional Block Diagram of the Dual Frequency Radar Data Processing, Analysis, and Display Equipments 16
4. Functional Block Diagram of the 10 cm Dual Frequency Doppler Radar Coherent Frequency Source 17
5. Typical Single Sideband Phase Noise of the 1120S Quartz Oscillator 18
6. 30 MHz Reference Signal Before Filtering 19
7. 30 MHz Reference Signal After Filtering 19
8. Physical Layout of Coherent Drive Source 20
9. Simplified Block Diagram of PRT Generator 21
10. Simplified Schematic of the Modulator Conversions 22
11. Spectrum of Simultaneously Pulsed Transmitters 23
12. Diplexer Configuration 25
13. Powers in the Output and Load Arms of the Diplexer 25
14. Waveguide Configuration and Losses 26
15. TR Limiter 27
16. Effect of RF Amplifier Overloading on Reflectivity Channel Video 28
17. Block Diagram of the 10 cm Dual Frequency Receiver 29
18. Noise Source and 20 dB Crossguide Coupler 31
19. Simplified Block Diagram of Calibration Unit 33
20. Receiver Calibration Curves With and Without the RF Amplifier 34
21. 7.3-Meter Antenna 36
22. 7.3-Meter-Antenna Azimuth Radiation Pattern Without Radome 37
23. 7.3-Meter-Antenna Elevation Radiation Pattern Without Radome 37
24. AB-563 Tower With Extension and CW-860 Radome 38
25. Station Primary Power Distribution 40
26. Switchgear Master Control Panel 40

Tables

1. Characteristics of the Dual Frequency Doppler Radar 14
2. TR Limiter Characteristics 28
3. Attenuator Characteristics 32
4. Radome Characteristics 36

A 10 cm Dual Frequency Doppler Weather Radar

Part I: The Radar System

1. INTRODUCTION

This report summarizes functional design concepts for a new 10-cm band dual frequency Doppler weather radar developed at the Air Force Geophysics Laboratory. Much of the impetus for this effort arises from the joint need of the Departments of Commerce, Defense, and Transportation to evaluate Doppler weather radar methodologies that will reduce the risk to the government during the Next Generation Weather Radar (NEXRAD) system development. The intent of this development is to examine certain of these methodologies for their suitability in both research and operations.

In recent years, the development of techniques for alleviating range-velocity ambiguities in pulsed Doppler radar observations of severe storm phenomena has been pursued at several research organizations. Doviak et al[1,2] and the JDOP Staff[3] provide excellent summaries of the benefits and limitations of a variety of

---

(Received for publication 22 October 1982)

1. Doviak, R.J., Sirmans, D.S., Zrnic', D.S., and Walker, G.B. (1978) Considerations for pulse Doppler radar observations of severe thunderstorms, J. Appl. Meteorol. 17:189-205.

2. Doviak, R.J., Zrnic', D.S., and Sirmans, D.S. (1979) Doppler weather radar, Proc. IEEE 67:1522-1533.

3. JDOP Staff (1979) Final Report on the Joint Doppler Operational Project (JDOP) 1976-1978. NOAA Tech. Memo, ERL NSSL-86.

techniques for extending radar's maximum unambiguous range and velocity and thereby minimizing the effect of these ambiguities. Many factors may favor one approach over another for a given application, but from an overall radar system performance standpoint, probably no issue is more critical than the compatibility of the ambiguity reduction scheme with techniques for the reduction of the influence of ground clutter. In the design of the radar described in this report, primary emphasis is placed on the system performance in a clutter environment, and the technique used to extend the radar's unambiguous range and velocity span is an important, but secondary, consideration.

2. SYSTEM CONFIGURATION

Ground clutter and anomalous propagation effects are reduced in the AFGL radar system by a dual channel (in-phase and quadrature) three pole elliptic filter operating on uniformly spaced pulse trains (Groginsky and Glover[4]). This filter provides 50 dB clutter rejection in the band from 0 to ±0.3 m/sec and passes unambiguous velocities greater than 1 m/sec with the introduction of no more than 1 dB of ripple. The design of this all-range canceller is based upon three performance considerations. First, a continuous pulse train canceller does not impose a penalty in radar dwell time to compensate for the transient response of the filter, whereas such penalties are associated with their discontinuous cousins. The work of Hamidi and Zrnic'[5] suggests that even with the use of techniques for reducing transient effects, these penalties may be as great as a factor of 2 in dwell time for comparable performance in the velocity channel and 20 dB poorer performance in the variance channel. Second, the canceller is designed to operate with 8 bit A/D converters currently in use so that no more than 50 dB of clutter cancellation is possible. At many sites, however, 50 dB of cancellation effectively clears all ranges of ground clutter with the antenna one-way half power point on the horizon. The final point concerning the clutter canceller is that hardware considerations show that a 3-pole elliptic filter is the simplest configuration meeting the performance requirements presented above.

The range and velocity ambiguities are important in the design of a pulse Doppler weather radar, especially in the observation of severe storms. Conventional single-frequency pulse Doppler radars transmit a series of equally spaced

---

4. Groginsky, H. L., and Glover, K. M. (1980) Weather radar canceller design, Preprints, 19th Conference on Radar Meteor., Am. Meteor. Soc., Boston, Mass.

5. Hamidi, S., and Zrnic', D. S. (1981) Considerations for the design of ground clutter cancellers for weather radars. Preprints, 20th Conference on Radar Meteor., Am. Meteor. Soc., Boston, Mass.

pulses. As a result, the maximum unambiguous range and velocity are a function of the pulse repetition time (PRT) as seen in the following equations:

$$R_{MAX} = \frac{c(PRT)}{2} \quad (1)$$

$$V_{MAX} = \frac{\lambda}{4PRT} \quad (2)$$

where

R_{MAX} = Maximum Unambiguous Range

c = Velocity of Propagation

PRT = Pulse Repetition Time

V_{MAX} = Maximum Unambiguous Velocity

λ = Wavelength

It becomes apparent from Eq. (2) that the maximum unambiguous velocity is related to the wavelength and the PRT and since the wavelength is chosen by other considerations the PRT is the final determining factor. Large values of R_{MAX} and V_{MAX} are desirable; however, it can be seen that the PRT varies directly in Eq. (1) and inversely in Eq. (2), therefore, some compromise must be reached in conventional pulse Doppler radars employing a single PRT.

To capitalize on the effectiveness of continuous pulse ground clutter filtering, this radar minimizes range and velocity ambiguities by transmitting two frequencies (Figure 1) with different but uniform PRT's. This method enables simultaneous processing of reflectivity information in separate channels of the receiver. Since the pulse separation is constant for each channel, both clutter cancellation and pulse pair velocity estimation are effected with contiguous pulse returns. The two PRT's are selected so that one is of sufficient length to preclude range ambiguities in the reflectivity channel and the second is of sufficiently short duration to provide a reasonably wide unambiguous velocity measurement span. Because the reflectivity information is unambiguous in range, range-folded data in the velocity channel are assigned to the correct range on the basis of echo locations in the reflectivity channel. In cases where the range-folded velocity data from two echoes overlap, the velocity information is attributed to the stronger echo if the difference in reflectivity is greater than 10 dB, and both echoes are labeled indeterminate if the difference is less than 10 dB.

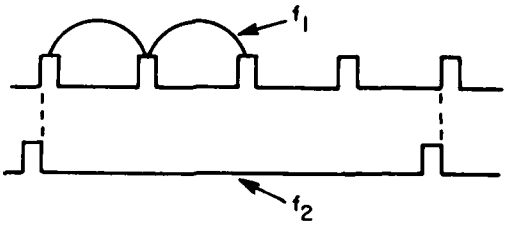

Figure 1. Transmitter Timing Sequence for the Dual Frequency Radar. The Doppler channel is f_1 and the reflectivity channel f_2

The functional form of the dual frequency radar is shown in Figure 2 and its characteristics are listed in Table 1. It consists of two separate transmitter-receiver chains which share a common antenna. Coherent frequency sources for the radar are derived from four phase locked oscillators (PLOs) which are referenced to a highly stable low-phase-noise quartz oscillator. A times-6 multiplier which provides the 30 MHz reference frequency for the linear receiver is also referenced to this oscillator. One PLO derives the frequency f_1 (2.710 GHz) for the velocity channel, and a second PLO derives the frequency f_2 (2.760 GHz) for the reflectivity channel. The third and fourth PLOs generate the local oscillator frequencies for the velocity and reflectivity channel mixer-preamplifiers. Each transmitter chain, which consists of the PLO, a traveling wave tube amplifier, and a Klystron amplifier, produces 1.2 MW rf pulses of 1 μsec duration. The rf pulses from each transmitter are combined in a diplexer and sent, via a circulator and waveguide switch, to the antenna.

Received signals at both transmitter frequencies are amplified in a wideband rf amplifier and then split equally in power into two channels, one for velocity and the other for reflectivity. Uniformly spaced velocity information is sent to the original Pulse Pair Processor (Novick and Glover[6]) where the gain is automatically controlled and the clutter cancelled, before the information enters the fault tolerant weather radar processor (FTWRP). Well calibrated reflectivity channel information enters the FTWRP directly. The FTWRP (Jagodnik et al[7])

---

6. Novick, L.R., and Glover, K.M. (1975) Spectral mean and variance estimation via pulse pair processing. Preprints, 16th Conference on Radar Meteor., Am. Meteor. Soc., Boston, Mass.

7. Jagodnik, A.J. Jr., Young, M.J., Banis, K.J., and Glover, K.M. (1980) A programmable fault-tolerant meteorological radar signal processor, Vol. 8, 1980 Digest of Papers, Gov't Microcircuit Appl. Conf., Naval Electronic Sys. Command, Washington, D.C.

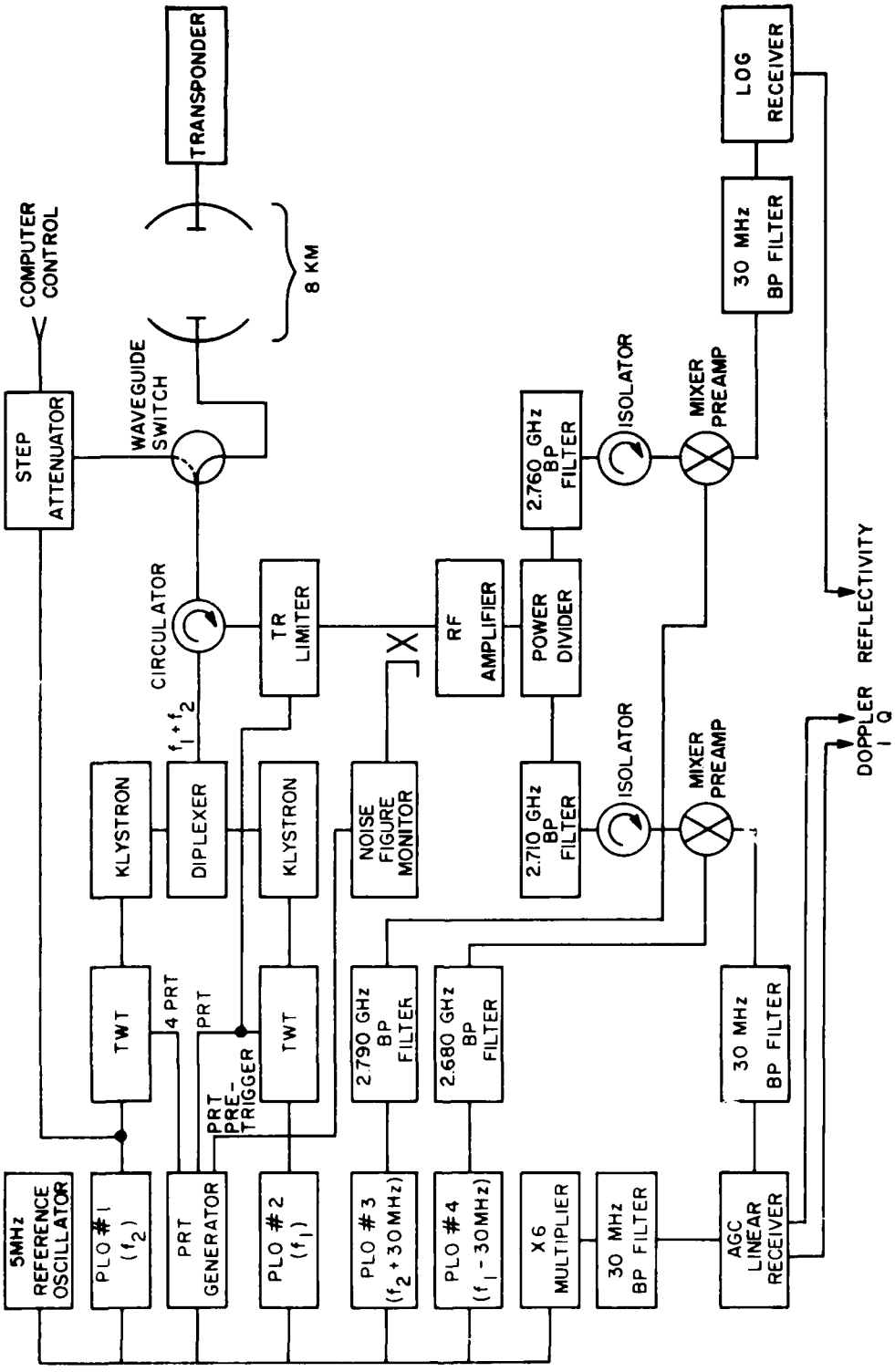

Figure 2. Functional Block Diagram of the 10 cm Dual Frequency Doppler Radar Transmitting and Receiving Equipments

Table 1. Characteristics of the Dual Frequency Doppler Radar

Transmitter	
Frequency f_1–Doppler	2.710 GHz
Frequency f_2–reflectivity	2.760 GHz
Peak power (f_1 and f_2)	1.2 MW
Pulse width (f_1 and f_2)	1.0 μsec
Pulse repetition time (f_1 and f_2)	768 μsec to 10 msec
Antenna	
Diameter	7.3 m
Gain	43.8 dB
Beamwidth–azimuth	1.0 deg
Beamwidth–elevation	1.0 deg
Waveguide losses–transmit	2.25 dB
Waveguide losses–receive	3.35 dB
Scan angle–azimuth	0-360 deg
Scan angle–elevation	0-90 deg
Scan type	continuous
Scan control	computer
Scan rate	15 deg/sec max
Acceleration rate	15 deg/sec^2
Azimuth and elevation accuracy	0.05 deg static error
Receiver	
Minimum detectable signal (f_2)	-111 dBm
Unambiguous range (f_1)	115 km
Unambiguous range (f_2)	461 km
Usable range (f_1)	230 km
Unambiguous velocity span (f_1)	±36 m/sec
Receiver noise figure	2.5 dB
Receiver bandwidth (f_1 and f_2)	1.1 MHz
Dynamic range with rf amplifier (f_2)	80 dB
Dynamic range without rf amplifier (f_2)	86 dB
Saturation level with rf amplifier (f_2)	-30 dBm
Saturation level without rf amplifier (f_2)	-10 dBm

is a self-repairing programmable signal processor which utilizes a distributed array of identical programmable computers-on-a-card with an internal architecture and instruction set optimized for signal processing. Each card is programmed to simultaneously implement a partitioned set of data processing instructions, and a hierarchy of fault detection and fault tolerance procedures. The processor provides reflectivity estimates, pulse-pair estimates of velocity for each range cell to compute either radial or the tangential components of shear, and finally, assigns range folded velocity echoes to their proper range.

Reflectivity, mean radial velocity, and variance/tangential shear/radial shear estimates are passed to an encoder/decoder for simultaneous distribution to three major independently operated sub-systems: a magnetic tape archiving system, a four-channel color display, and a Perkin-Elmer Model 3242 computer. Except for the computer and the attendant high resolution color terminal, these equipments are identical to those described by Glover.[8] The present computer retains all of the features of its predecessor and also provides considerably improved capabilities for on-line analysis and operator interaction. A detailed description of the computer features is given in the Radar Monitor, Control and Evaluation System report. Figure 3 shows the functional block diagram of the dual frequency radar data processing, analysis, and display equipments.

3. SYSTEM DESCRIPTION

3.1 Transmitter

3.1.1 COHERENT FREQUENCY SOURCE

The coherent frequency source, shown in functional form in Figure 4, uses an Austion Type 1120S, 5 MHz quartz oscillator as its stable frequency source. The oscillator exhibits extremely low phase noise and has a short term stability, in the time domain, of 3×10^{-12} over a millisecond. Figure 5 is a plot of the oscillator's phase noise in a 1 Hz bandwidth. The harmonic distortion is 25 dB below the output frequency. The quartz resonator and oscillator circuit are enclosed in a solid-state proportional control oven, assuring noise-free temperature stabilization over a wide range of ambient temperatures. To properly distribute and isolate the 5 MHz frequency source, low noise buffer amplifiers are placed at the output of the oscillator.

8. Glover, K. M. (1980) On the automation of weather radar information for air and ground operations. Preprints, 19th Conference on Radar Meteor., Am. Meteor. Soc., Boston, Mass.

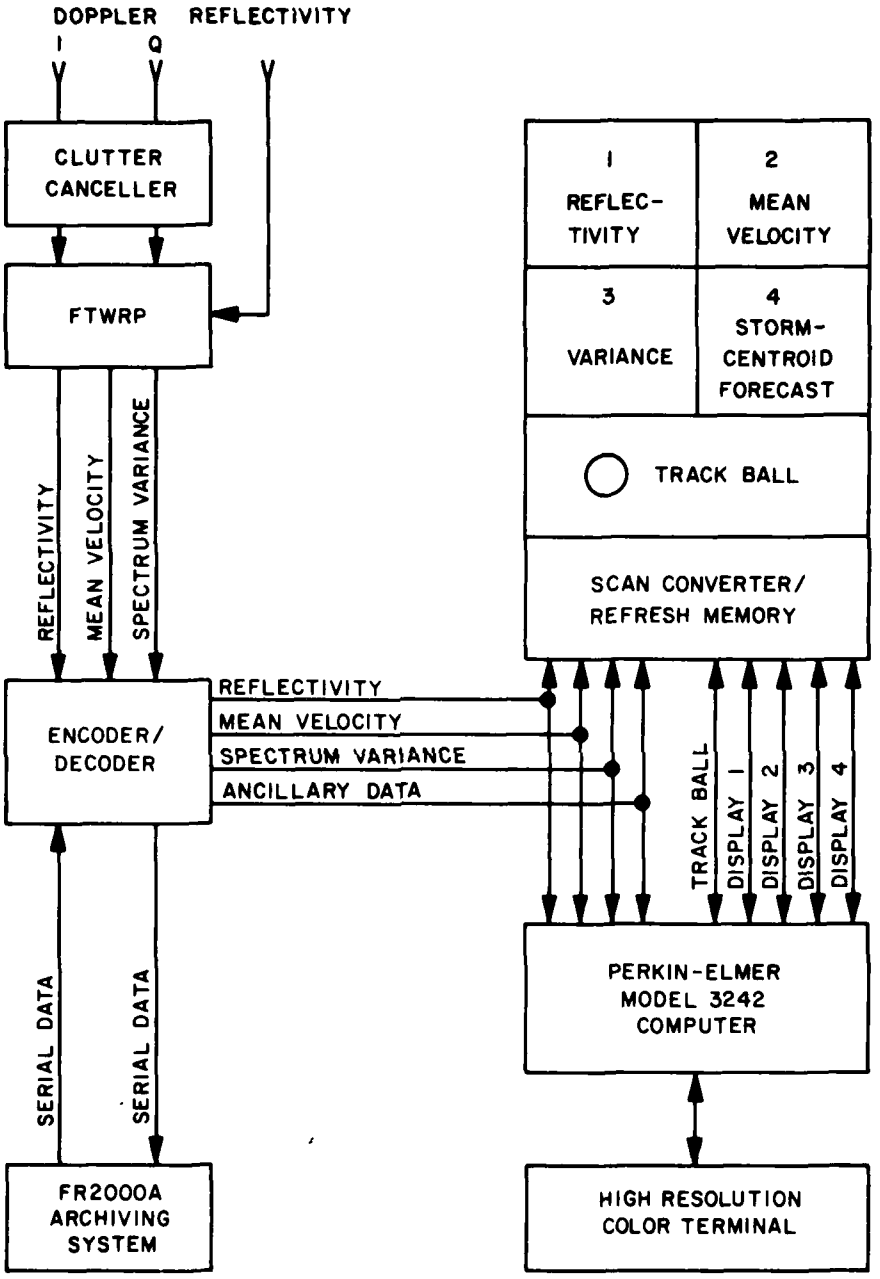

Figure 3. Functional Block Diagram of the Dual Frequency Radar Data Processing, Analysis, and Display Equipments

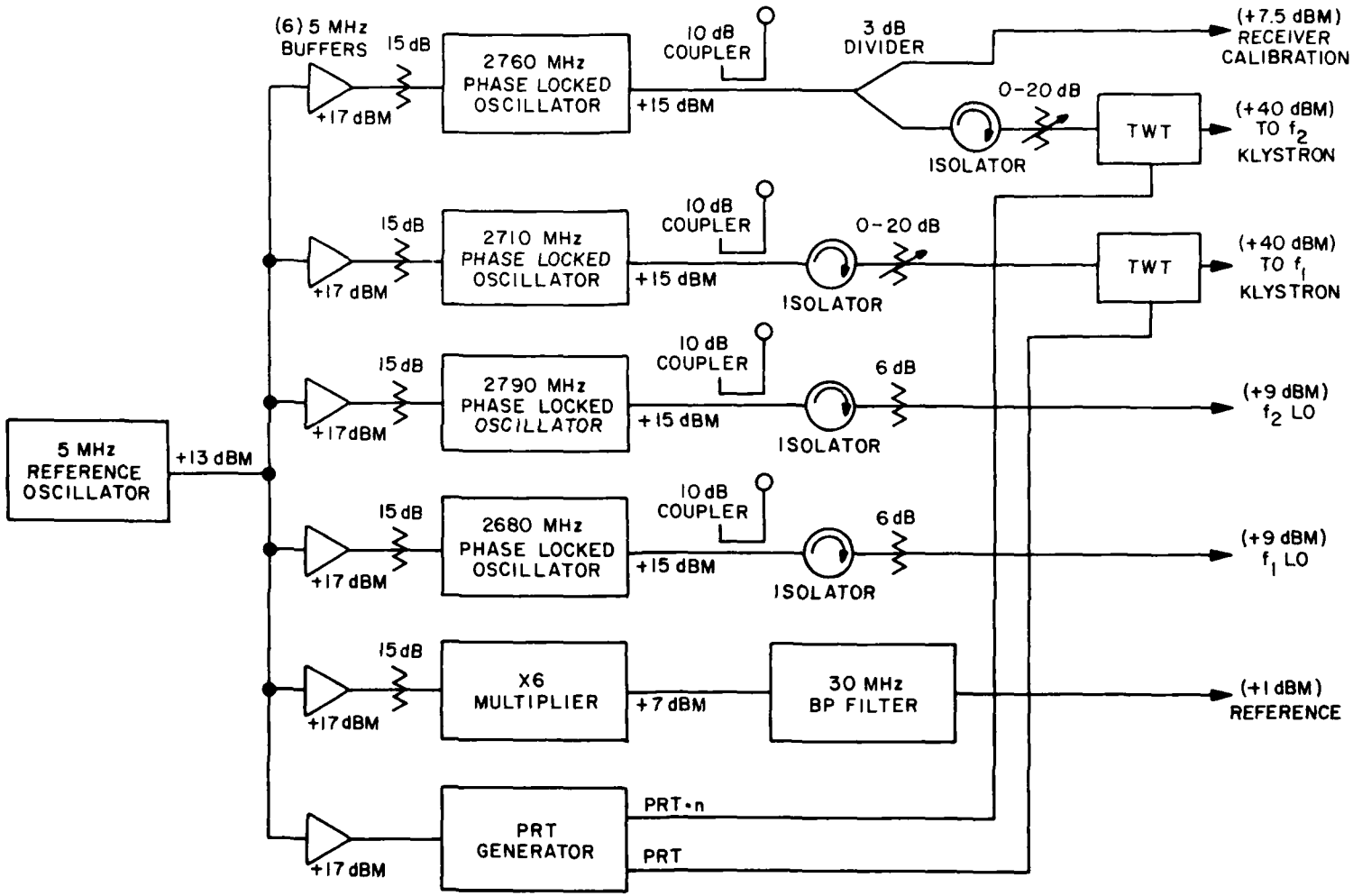

Figure 4. Functional Block Diagram of the 10 cm Dual Frequency Doppler Radar Coherent Frequency Source

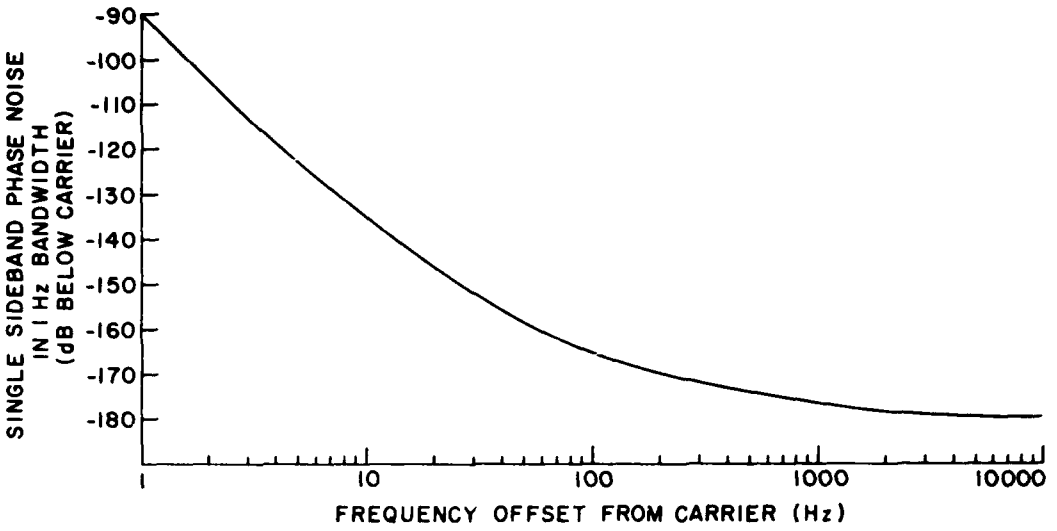

Figure 5. Typical Single Sideband Phase Noise of the 1120S Quartz Oscillator

Four phase locked oscillators (PLOs), with mechanically tuned cavities, are referenced to the 5 MHz quartz oscillator to derive phase coherent frequencies for the two transmitters and the receiver local oscillators. The +15 dBm output level of each PLO is isolated with a ferrite device, having a typical insertion loss of 0.3 dB, to prevent PLO instability due to mismatches caused by the traveling wave tube (TWT) amplifiers, which have a typical input VSWR of 2:1. The TWT provides drive power to the VA-87 Klystrons. Each PLO output is frequency monitored by the Quality Assurance/Fault Location Network which sequences a frequency counter through the PLO output couplers with a PIN diode switch. The reference signal (30 MHz) for the quadrature receiver used in the velocity channel is derived by multiplying the 5 MHz by a factor of 6. Since multipliers produce sidebands in addition to the desired output frequency, the 30 MHz reference frequency was passed through a filter with a 1 MHz bandwidth at the 3 dB points. Figure 6 shows a power spectrum of the unfiltered 30 MHz reference signal with the sidebands located at ±5 MHz intervals from the center frequency and only 30 dB down. Figure 7 shows the results after filtering, with all sidebands down by greater than 70 dB. The filtering of the 30 MHz reduces the possibility of contaminating the Doppler spectrum in the processing equipment.

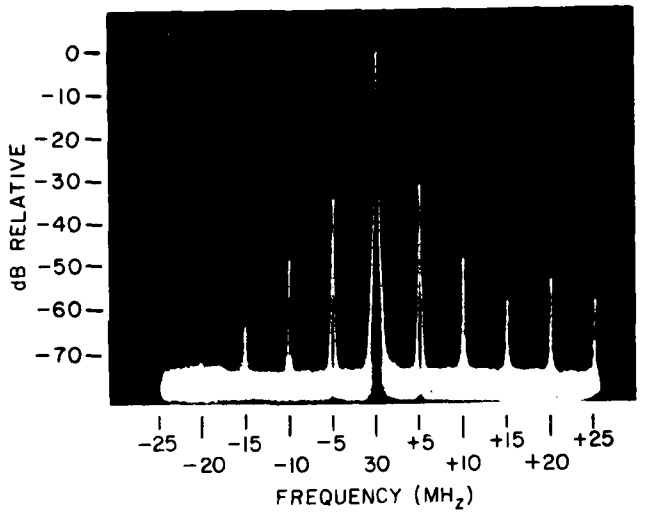

Figure 6. 30 MHz Reference Signal Before Filtering

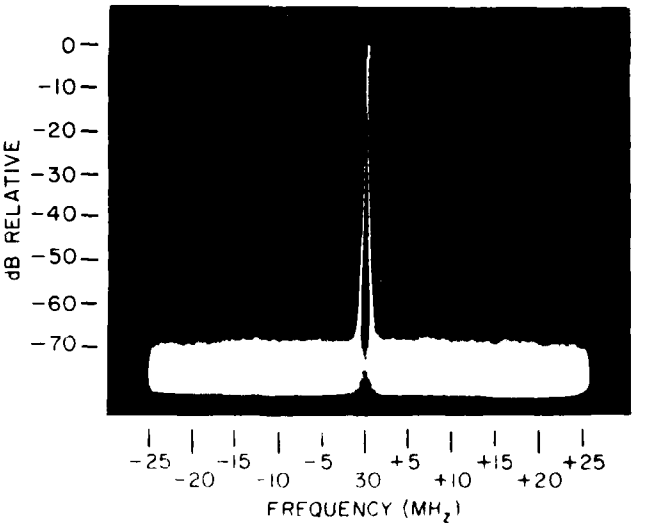

Figure 7. 30 MHz Reference Signal After Filtering

The physical layout of the coherent frequency source (Figure 8) shows the 5 MHz oscillator output and the buffered 5 MHz reference outputs at the extreme left with the 30 MHz reference and filter at the top center. The four PLOs are directly below the 30 MHz reference filter and at the lower right are two variable attenuators used to control the drive to the Klystrons. To prevent coherent source leakage from contaminating the receiver, solid jacketed coaxial cable was used throughout the unit.

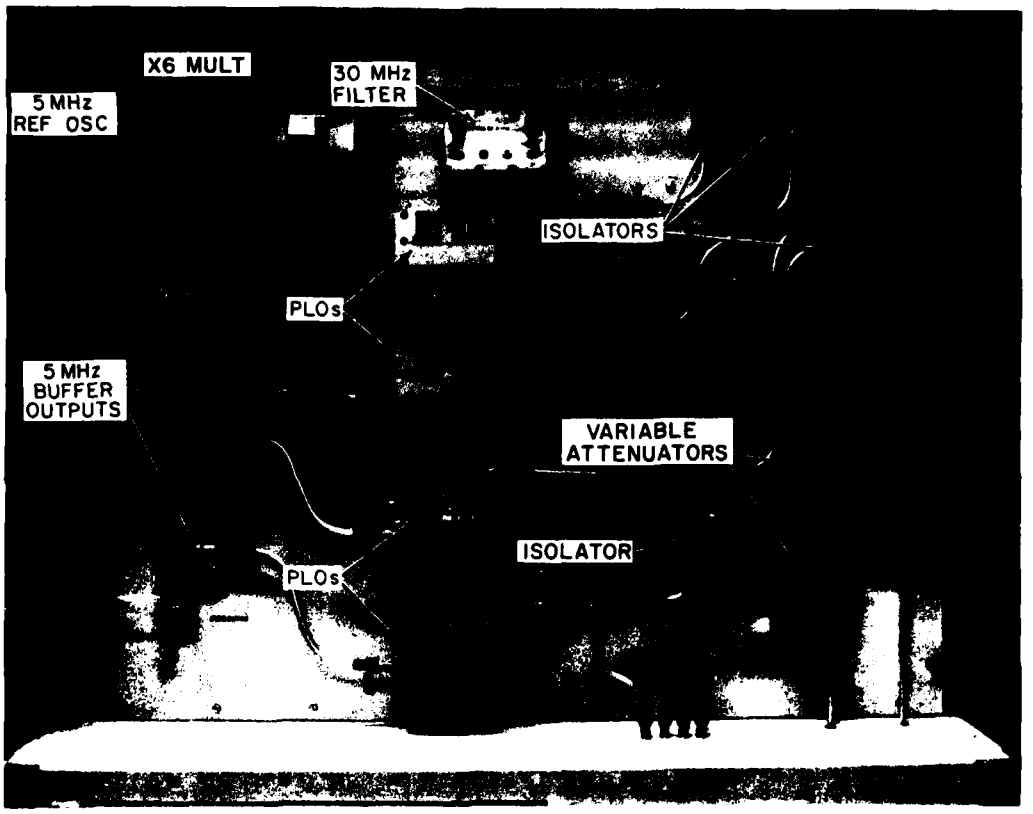

Figure 8. Physical Layout of Coherent Drive Source

3.1.2 PULSE REPETITION TIME GENERATOR (PRT)

Referencing the PRT generator to the 5 MHz oscillator avoids the problem of spurious mixer products[9] in the receiver, and also provides a convenient source for the generation of a stable pulse train with the time resolution required. The

9. Taylor, J.E., and Mattern, J. (1970) Radar Handbook, McGraw Hill, New York, Chapter 5, pp 15-16.

PRT generator is designed to have an adjustable pulse repetition time in 1 μsec intervals and produces two pulse repetition times, one being a submultiple of the other. This feature allows the choice of a PRT that matches the number of range cells processed and the associated delays in the digital processing equipment without wasted deadtime.

In the simplified block diagram (Figure 9) of the PRT generator the reference oscillator is divided by a factor of 5 to produce a 1 MHz pulse train which is then counted in BCD. The output of the counter is compared to either a BCD thumbwheel switch value or a preset fixed code as determined by a selector switch located on the circuit board. The counter is reset when it reaches the selected value and the procedure is then repeated. The resultant trigger is then sent to the velocity channel and also divided by factors of 1, 2, 3, or 4, one of which is selected by a

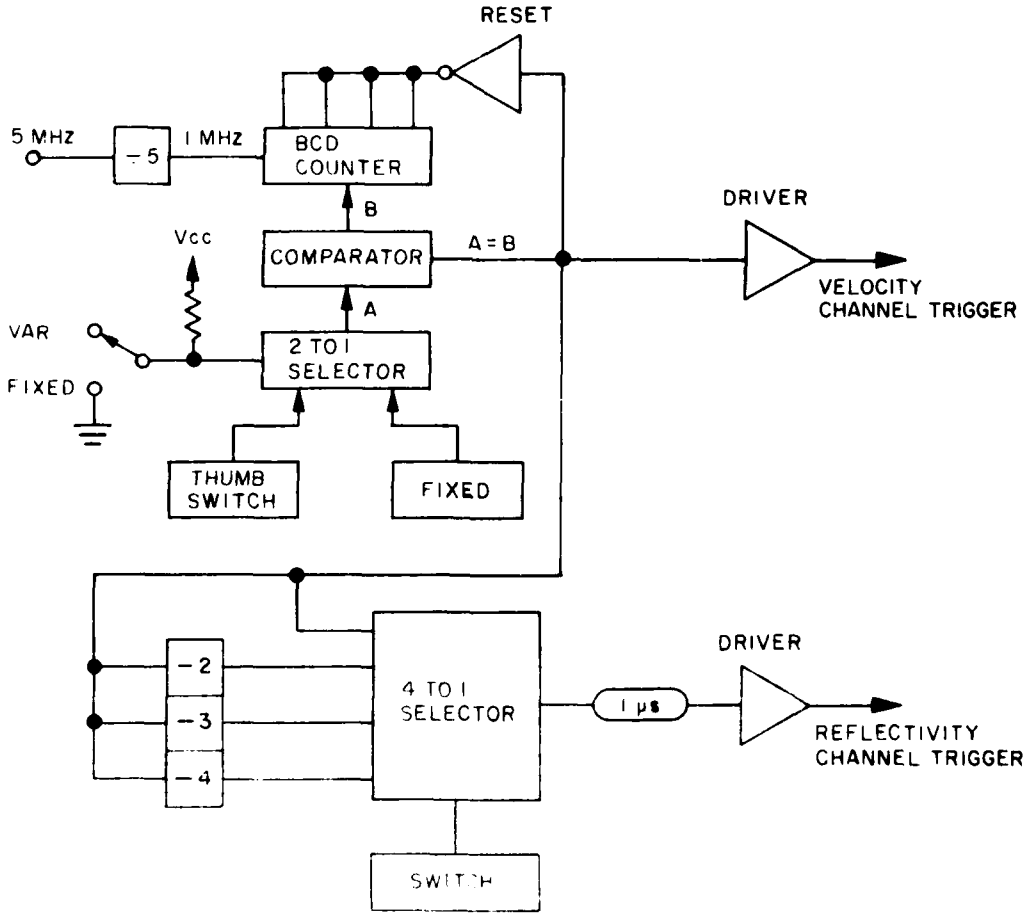

Figure 9. Simplified Block Diagram of PRT Generator

front panel switch. The divided pulse train is delayed in time by 1 μsec and triggers the reflectivity channel transmitter. The purpose of the delay is to avoid the modulation products that would be radiated by simultaneously pulsing the two transmitters. A more detailed description of the modulation products which are radiated with simultaneous transmission is covered in Section 3.1.3. The versatility of this generator allows the selection of PRTs from 768 μsec to 10 msec in 1 μsec increments. The minimum PRT, of course, is limited by the maximum transmitter duty cycle.

3.1.3 TRANSMITTERS

Since the concept of a dual frequency radar using two separate transmitters does not make serious operational demands on either transmitter, two surplus FPS-18 transmitters were used as the base upon which to build. The FPS-18 is a 1959 vintage radar with a line type modulator pulsing a Varian VA-87 Klystron. In order to modernize the transmitters and increase their reliability, all vacuum tube diodes in the modulator and high voltage power supplies were replaced with solid state versions. A simplified schematic of the modulator conversion is shown in Figure 10.

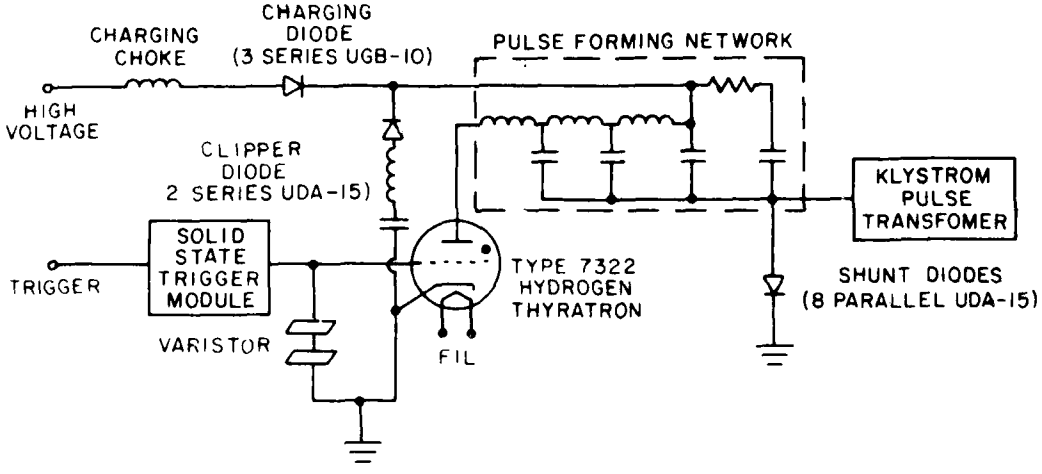

Figure 10. Simplified Schematic of the Modular Conversions

The original trigger amplifier, a Vacuum Tube Line type modulator requiring 5 kV, 800 V and 300 V power supplies and the 1257 hydrogen thyratron, which required a critical reservoir adjustment, were replaced with a solid state trigger

module and a 7322 ceramic-metal hydrogen thyratron. The reservoir in the new thyratron is connected to the heater and does not require adjustment. Two varistors are placed in the grid circuit of the thyratron to eliminate the large voltage spikes associated with these tubes. These voltage spikes cause voltage breakdowns between the grid and the ground plane.

Both transmitters have over 200 h of trouble free operation with peak output powers of 1.2 MW each at 1 μsec pulse width over PRTs from 768 μsec to 10 msec. The transmitters are pulsed 1 μsec apart but can be operated contiguously. Although the system has the power handling capability to pulse both transmitters simultaneously, unwanted modulation products are produced by nonlinearities in the diplexer and are radiated. These modulation products occur at 50 MHz intervals, the interval being a function of the difference frequency of the transmitters. The spectrum radiated during simultaneous operation is shown in Figure 11 with the modulation products at frequencies of 2610, 2660, and 2810 MHz. These products are only 40 to 50 dB below the carrier frequencies and although they are not detected by the receiver they do contaminate an already crowded frequency band.

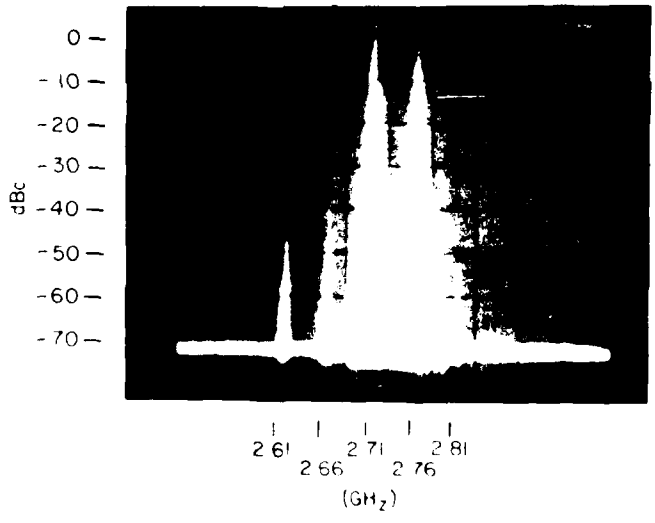

Figure 11. Spectrum of Simultaneously Pulsed Transmitters

3.2 RF Transmission

3.2.1 DIPLEXER

Since both transmitters would share a common waveguide and antenna, a device that would combine the two frequencies (f_1 and f_2) was needed. Teeter and Bushore[10] developed a power splitter that operated at a wavelength of 3 cm. It became apparent that if the input and outputs were reversed a 10 cm version could be constructed that would perform as a diplexer and would handle the high transmitted peak power and be reasonably small (physically). Other attributes of this device are its low insertion loss, its independence of the pulse timing, its isolation between transmitters and its wide bandwidth.

For maximum coupling of the frequencies f_1 and f_2 into the output port of the diplexer (Figure 12) the difference length "d" in waveguide No. 2 must provide an integral number of wavelengths at f_1 and an odd multiple of a half guide wavelength of f_2. Therefore, "d" is the minimum additional length needed in waveguide No. 2 in order to establish the correct phase relationship between frequencies f_1 and f_2. Calculation for the length "d" is given by Eq. (3).

$$d = \frac{\lambda_{g1}\lambda_{g2}}{2(\lambda_{g1} - \lambda_{g2})} \tag{3}$$

where

d = added length of waveguide no. 2

λ_{g1} = guide wavelength of f_1

λ_{g2} = guide wavelength of f_2 (the higher frequency)

One of the predominant factors in choosing a frequency separation of 50 MHz for the dual frequency radar was to keep the physical length d reasonable. From Eq. (3) it can be seen that the length d increases rapidly as the frequency separation decreases.

Isolation between transmitters has a measured value of 34 dB. The isolation achieved depends on the input hybrid coupler. Insertion loss of the diplexer at both f_1 and f_2 is 0.1 dB with a measured VSWR of 1.12:1 at f_1 and 1.14:1 at f_2. Plots of the powers in the output and load arms of the diplexer, as a function of frequency, are shown in Figure 13.

10. Teeter, W.L., and Bushore, L.R. (Lt. Cdr.) A Dual-Frequency Microwave Diplexer. Head, U.S. Naval Electronics Lab Report No. [illegible].

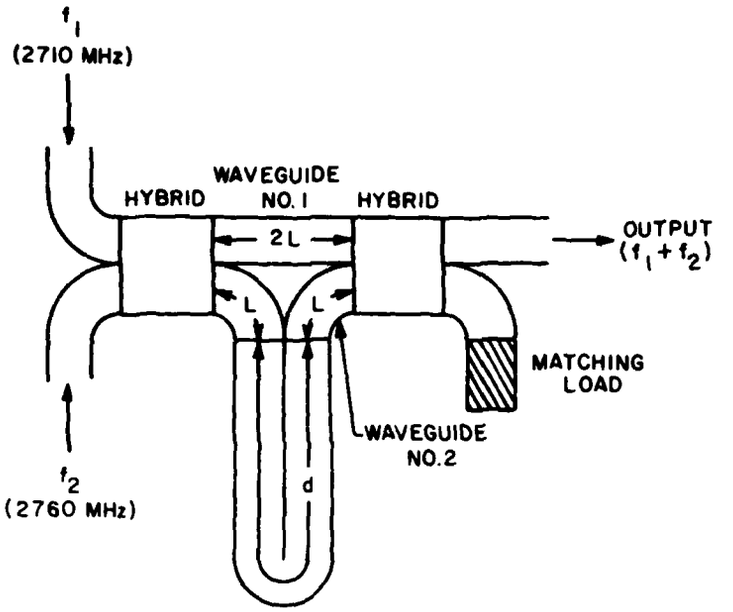

Figure 12. Diplexer Configuration

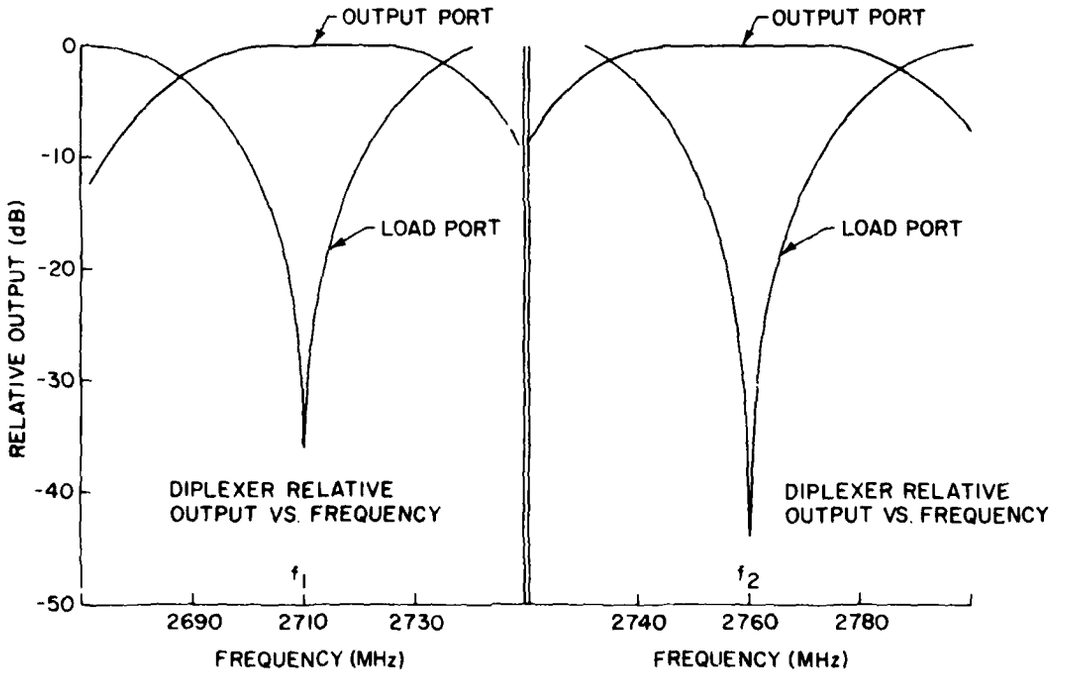

Figure 13. Powers in the Output and Load Arms of the Diplexer

3.2.2 HIGH POWER CIRCULAR AND DIRECTIONAL COUPLERS

Energy from the two transmitters at the diplexer output is sent into a differential phase shift circulator which has a power handling capability of 5 MW peak and 4 kW average. The circulator has an insertion loss, in the transmit path, of 0.35 dB with an isolation between the transmit and receiver ports of 35.3 dB.

Three dual directional couplers, each having 60 dB attenuation in the forward direction and 35 dB attenuation in the reverse, are used for power measurements. Two are located at the output of the transmitters and the third is placed after the circulator where it is used to measure the forward and reverse power for computing the VSWR in the Quality Assurance/Fault Location Network. A fourth coupler, a dual 40 dB attenuation unit, is used to inject a calibrating signal from the radar transponder when operated locally. A simplified version of the waveguide configuration and associated losses is shown in Figure 14.

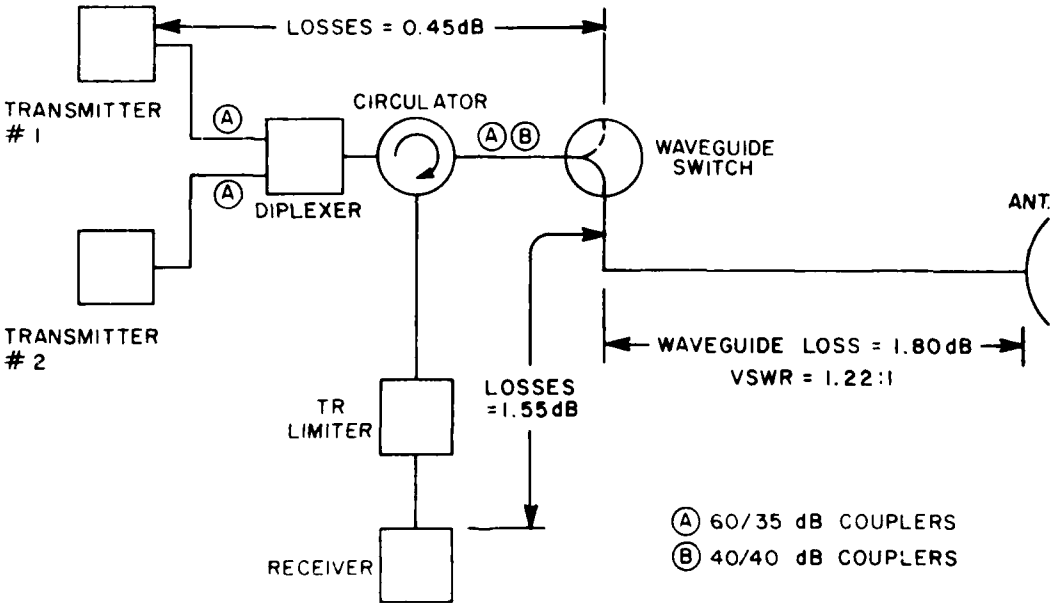

Figure 14. Waveguide Configuration and Losses

3.2.3 TR LIMITER

The TR limiter used in this system is shown in Figure 15 and is of the passive type requiring neither ignitor bias nor shutter. It consists of a pre-TR to handle transmitter overloads, a limiter, and a PIN diode attenuator. The PIN diode attenuator prevents the receiver rf amplifier from overloading by providing an

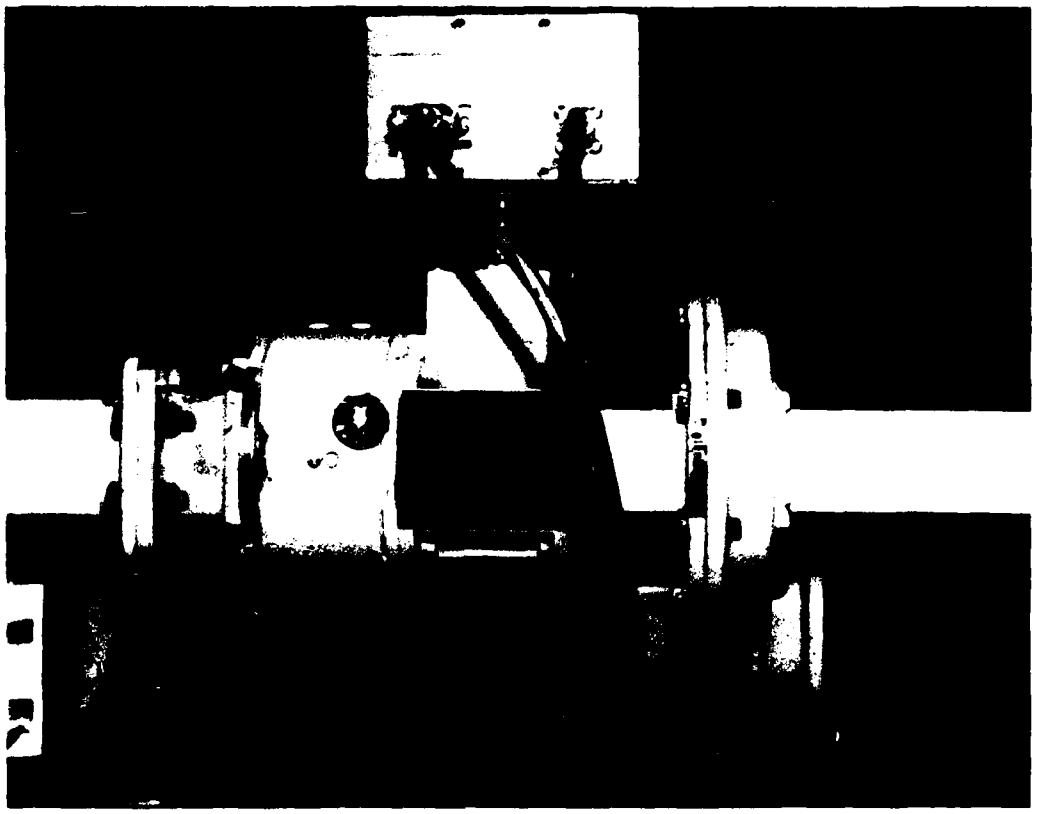

Figure 15. TR Limiter

additional 36 dB of attenuation during the transmit time. Without this PIN diode the rf amplifier recovery time is on the order of 600 μsec. Figures 16a and b show the reflectivity channel video with and without the PIN diode attenuator. The amplifier gain in Figure 16a increases in an exponential fashion similar to a sensitivity time control (STC). In Figure 16b the amplifier gain recovers in 3 μsec.

The pertinent characteristics of the TR limiter are shown in Table 2.

3.2.4 WAVEGUIDE ARC DETECTION

To protect the high power Klystron (VA-87B) pressure window from fracturing due to arcing within the waveguide, solid state electro-optical arc sensors are installed in each transmitter to detect visible arcs. The sensing portion is an integral part of a 90-degree waveguide bend located between the Klystron output flange and the waveguide transmission line. The output of each arc sensor is monitored by the Quality Assurance/Fault Location Network which disables the transmitters after a predetermined number of arcs occur and flags the fault.

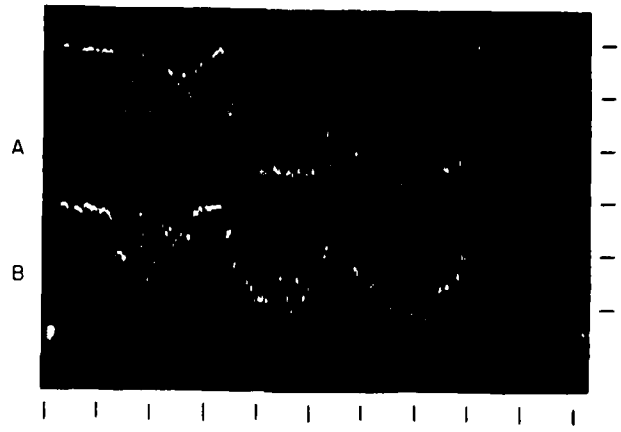

Figure 16. Effect of RF Amplifier Overloading on Reflectivity Channel Video. Trace A shows recovery without the P/N diode; Trace B, with the PIN diode

Table 2. TR-Limiter Characteristics

Frequency Band	2.7-2.9 GHz
Peak Power	150 kW
Average Power	200 W
Spike Leakage	0.5 W
Flat Leakage Power	50 mW
Recovery Time	3 μsec
Insertion Loss	0.1 dB
Low Level VSWR	1.4 to 1
PIN Diode Attenuation	36 dB

3.3 Receiver

3.3.1 DUAL FREQUENCY RECEIVER

The main design objectives for the receiver were that it exhibit a high degree of isolation between channels, sufficient sensitivity to detect weak weather targets, and have a dynamic range of at least 80 dB. The receiver, shown in block diagram form in Figure 17, was designed and built in-house using commercially available modules.

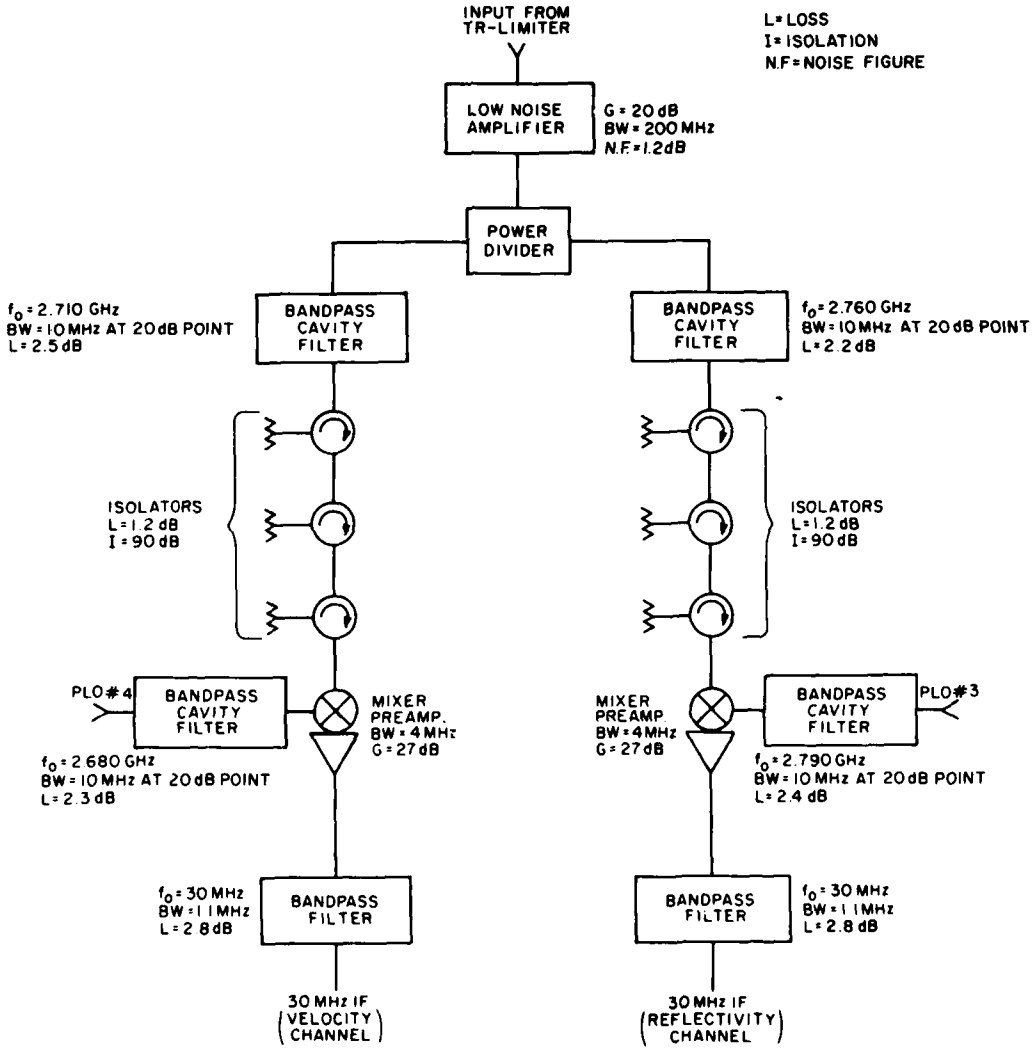

Figure 17. Block Diagram of the 10 cm Dual Frequency Receiver

Received signals at both transmitted frequencies are amplified in the rf amplifier. This amplifier is extremely stable; has input level protection; and exhibits a noise figure of 1.2 dB over the 2700 to 2900 MHz frequency band, a gain of 20 dB, an input and output VSWR of 1.5:1, and a maximum output power of +10 dBm for 1 dB of compression. Signals, after rf amplification, are then power-split into two channels, one for reflectivity and the other for velocity. In order to prevent harmful sidebands from being generated in the quiet mixer-preamplifiers, the two mixers are isolated from each other by more than 200 dB at both the rf and IF. This degree of isolation is achieved by using bandpass cavity filters that have a 20 dB bandwidth of 10 MHz. These filters, centered at 2710 MHz and 2760 MHz, reduce the interference of the adjacent channel by 50 dB. Isolators placed between the cavity filter and mixer input provide 90 dB of isolation with a 1.2 dB total insertion loss. Isolation is maximized by selecting the isolator's third port termination to best match the operating frequency. After being equally divided in power, rf signals are filtered and isolated, then enter an image rejection quiet mixer where they are mixed with the appropriate PLO to form a heterodyned signal at the intermediate frequency of 30 MHz. The outputs of the phase locked oscillators are filtered with bandpass filters of the type used in the rf input section. They suppress the 5 MHz sidebands, inherent in the PLOs, to better than 90 dB below the carrier. Each quiet mixer preamplifier has a 3 dB bandwidth of 4 MHz with an rf to IF gain of 27 dB, a noise figure of 6 dB, and an output power of +10 dBm at the 1 dB compression point. The output from each mixer, prior to IF amplification, is filtered with a response approximating a Gaussian shape. This filter is slightly wider in bandwidth than a matched filter to reduce the time for recovery from impulse interference with no more than a 0.5 dB degradation in detectability from a matched filter. For the reflectivity channel, the IF amplifier provides a uniform logarithmic response ±1/2 dB over 80 dB dynamic range, and the Doppler channel amplifier uses automatic gain control at each range cell to provide a linear response over an 80 dB dynamic range.

3.3.2 RECEIVER NOISE FIGURE

The reflectivity receiver noise figure is measured with a solid state noise source using an AILTECH Type 7370 system noise monitor. This noise source is capable of performing both manual and automatic noise figure measurements. The noise source and the 20 dB crossguide coupler injecting the noise signal into the receiver waveguide can be seen in Figure 18. The noise figure is measured automatically by pulsing the noise source "on" 20 μsec prior to the next reflectivity transmission. The system noise monitor furnishes modulated low level DC power to the noise source, which in turn provides alternating noise-on and noise-off periods to the receiver. The receiver IF signal, consisting of periods

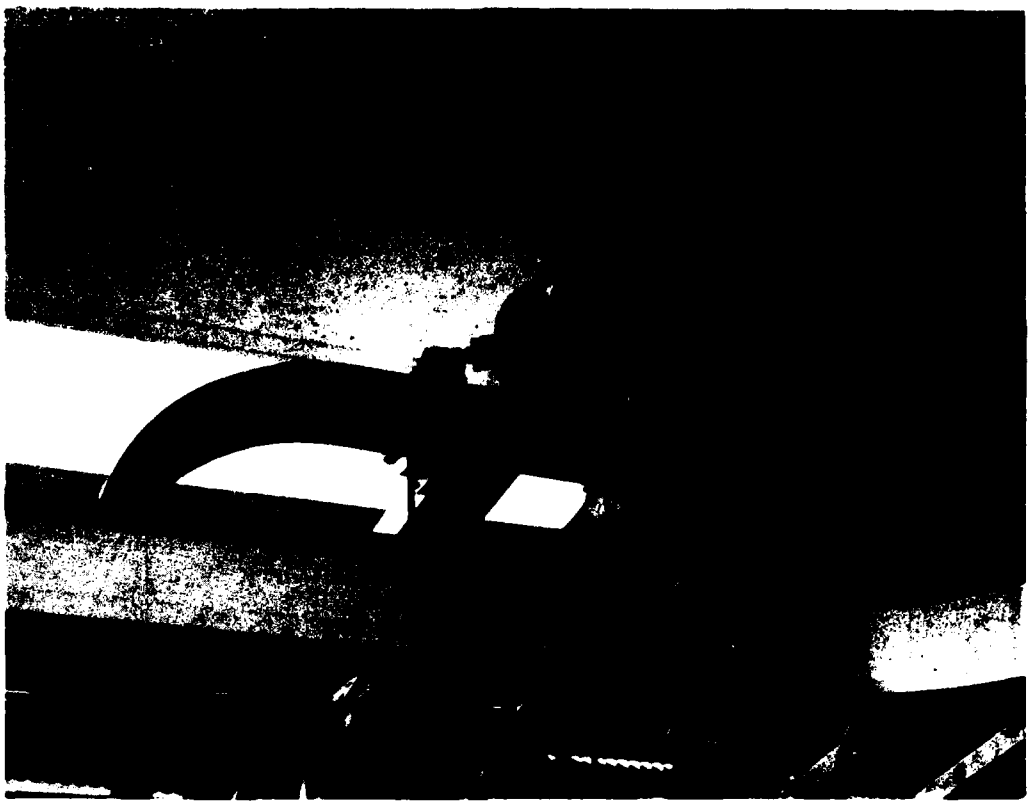

Figure 18. Noise Source and 20 dB Crossguide Coupler

of IF noise alone, alternating with periods of IF noise plus that added by the noise source, is applied to the system noise monitor input. The difference between the two detected levels derived from the IF signal is related to the noise performance of the receiver. This difference is synchronously detected and displayed directly as noise figure by the system noise monitor. Noise figure measurements of the system receiver were measured with the AILTECH system and a 2.5 dB noise figure was obtained.

3.3.3 CALIBRATION

3.3.3.1 Receiver

In order to provide repeatable, fast, and accurate receiver step calibrations, the entire process is accomplished with the aid of a computer. The computer provides a printout of dBm values versus the bit count number from the reflectivity channel, performs a linear regression analysis between the -30 dBm and -105 dBm

points, and provides a plot of the best fit line through these points. A detailed description of the computer operation and software required is presented in Volume III of this report "Radar Monitor, Control, and Evaluation System (RAMCES)".

The step attenuator required for this calibration can be programmed remotely, has low power and temperature coefficients, and has good repeatability. Table 3 shows the attenuator characteristics.

Table 3. Attenuator Characteristics

Range	0-121 dB
Increments	1 dB
Power Coefficient	0.0001 dB/dB (C^{o})
Temperature Coefficient	0.001 dB/dB (C^{o})
Repeatability	0.02 dB

Figure 19 is a simplified diagram of the receiver step calibration system. Binary Coded Decimal (BCD) signals representing dB values from the computer or a manually controlled thumbwheel switch are selected and converted to a 1-2-4-4 code to drive the attenuators. The 2760 MHz signal from the coherent driver is equally power divided and adjusted until the power meter, at the junction of the power divider, measures a calibrated reference level that provides a 0 dBm signal level at the waveguide switch. The power meter is set to a level that accounts for all the losses between it and the point of injection. Additionally the calibration reference level is constantly monitored and recorded during calibration by the computer via the power meter's BCD output.

Microswitches in the waveguide switch housing determine its position and control the transmitter so that radiation is not possible when the waveguide switch is in the calibrate position. The computer controls the position of the switch and the status lines signal the switch's position to the computer.

The receiver is isolated from the calibration source during transmitter operation by the maximum attenuator value of 121 dB and the waveguide switch isolation of 90 dB for a total isolation of 211 dB. Figure 20 is a comparison of receiver calibration curves with and without rf amplification. The plot of the receiver response with the rf amplifier shows a linear response in dB down to -110 dBm for an improvement of 14 dB in sensitivity. While the improvement is significant,

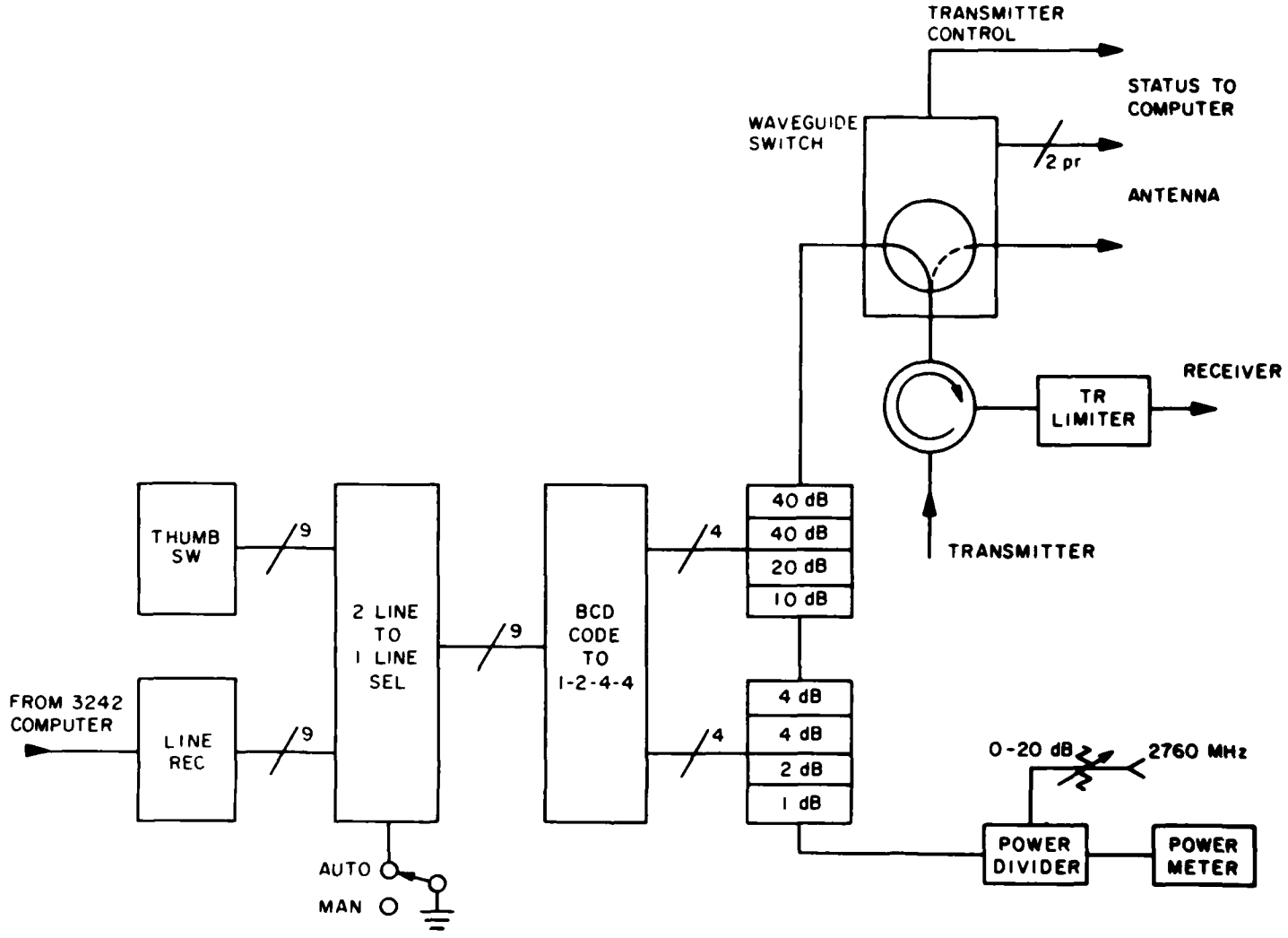

Figure 19. Simplified Block Diagram of the Calibration Unit

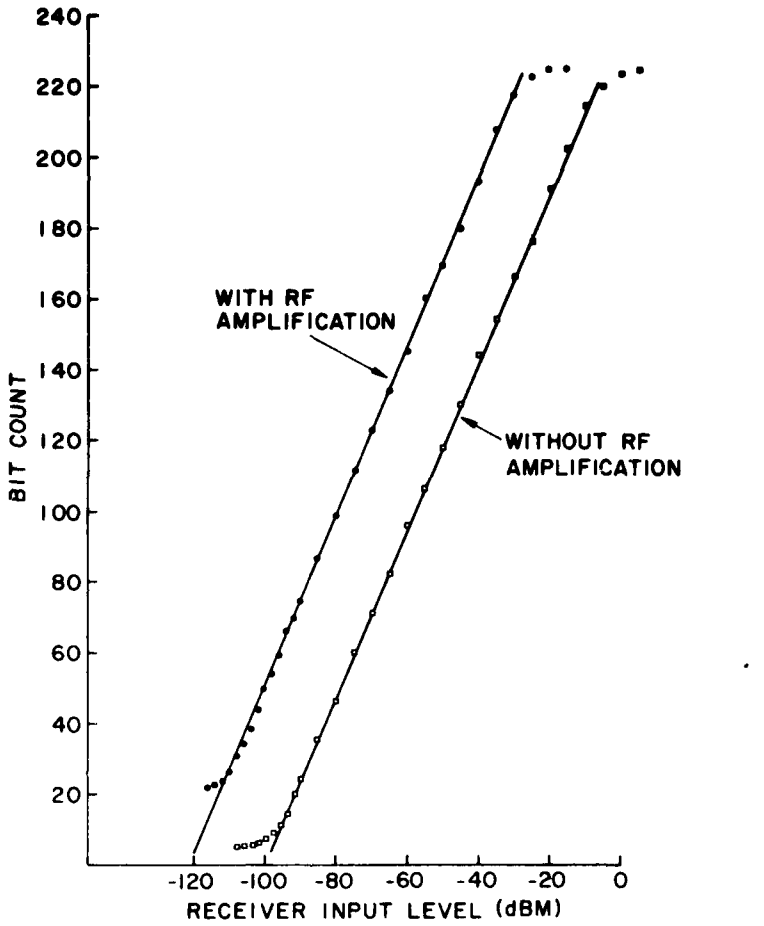

Figure 20. Receiver Calibration Curves With and Without the RF Amplifier

the amplifier with its 20 dB gain limits the saturation point to -30 dBm and the dynamic range to 80 dB. Without the amplifier the receiver has a saturation level of -10 dBm and a dynamic range of 86 dB.

3.3.3.2 System

During operations, a total calibration of the reflectivity channel is obtained through the use of a coded radar transponder (Glover et al[11]) and an associated 2760 MHz band pass filter that are located on a boresight tower approximately

11. Glover, K.M., Branche, J.R., Turner, J.H., and Groginsky, H.L. (1976) Precise calibration of coherent and non-coherent weather radars by means of a radar transponder. Preprint, 17th Conf. on Radar Meteor., Am. Meteor. Soc., Boston, Mass.

8 km from the radar. At those times when the main lobe of the radar antenna is aligned with the transponder antenna, 2760 MHz pulses from the radar trigger the transponder, which then generates a binary word signifying the power level received. This binary transmitter calibration code is delayed in time to correspond to an area devoid of other echoes and is retransmitted to the radar using frequency F_2. The power level of the coded transmission is alternated slowly in time to provide two receiver calibration signals spaced 20 dB apart. Signals received at the radar are processed through the reflectivity receiver and data processor in the same manner as any target return. The computer decodes the binary word to determine the transmitter power and measures the received power level to derive the receiver calibration. Since these calibrations involve the two-way transmission through the radome of the radar, this technique provides a true system calibration that includes attenuation due to the radome itself.

3.4 Antenna and Radome

The antenna used with the dual frequency Doppler weather radar, shown in Figure 21, is a 7.3-m-diameter solid parabolic reflector that is illuminated with a prime focus vertically polarized feed horn. The gain of this antenna is 43.8 dB, and it has a beamwidth in both azimuth and elevation of 1.0 deg, which is the antenna beamwidth necessary for the detection of a mesocyclone at 230 km.[3] The azimuth and elevation radiation patterns, showing the sidelobes more than 22 dB down, can be seen in Figures 22 and 23. The antenna is mounted on an elevation-over-azimuth tracking pedestal assembly capable of scanning continuously in azimuth and 0-90 deg. in elevation. Scan control of the antenna can be controlled manually or by computer. The maximum acceleration rate for this system is 15 deg/sec^2.

The entire antenna and pedestal assembly is mounted on a standard USAF type AB-563/GPS tower with a 7.6 m extension, placing the pedestal base 15 m above ground. A 17-m type CW-860 aluminum random-space-frame radome provides antenna operation with winds to 240 km/h. Each panel is covered with an ESSCOLAM^{TM*} membrane bonded to the welded aluminum framework. The membrane is protected by a Tedlar film that is an integral part of the membrane laminate structure. Typical electromagnetic characteristics[12] for the 17-m metal random-space-frame radome are listed in Table 4.

---

*ESSCOLAM^{TM} is a trademark of Electronic Space Systems Corp. (ESSCO) for its proprietary reinforced plastic membrane laminate.

12. Callahan, M.A. (1980) Technical manual TM79-29, Electronic Space Systems Corp.

Figure 21. 7.3-Meter Antenna

Table 4. Radome Characteristics

1. Transmission Loss, dB = 0.75 ONE WAY
2. Noise Temperature, K (Zenith) = 2.5
3. Boresight Shift (mrad, RMS) = 0.026
4. Sidelobe Perturbation = 1 dB AVG at -25 dB power level with antenna gain >45 dB

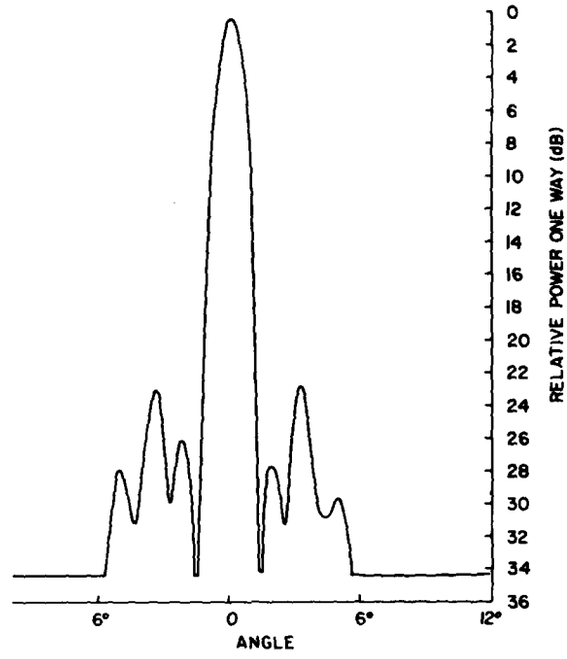

Figure 22. 7.3-Meter-Antenna Azimuth Radiation Pattern Without Radome

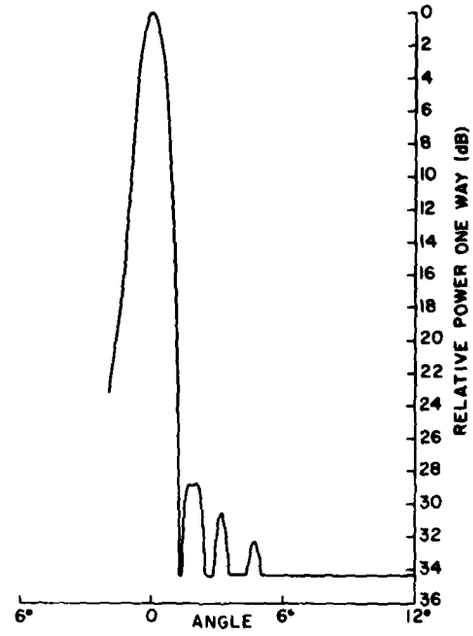

Figure 23. 7.3-Meter-Antenna Elevation Radiation Pattern Without Radome

The CW-860 radome atop the AB-563/GPS tower with its 7.6 m extension is shown in Figure 24.

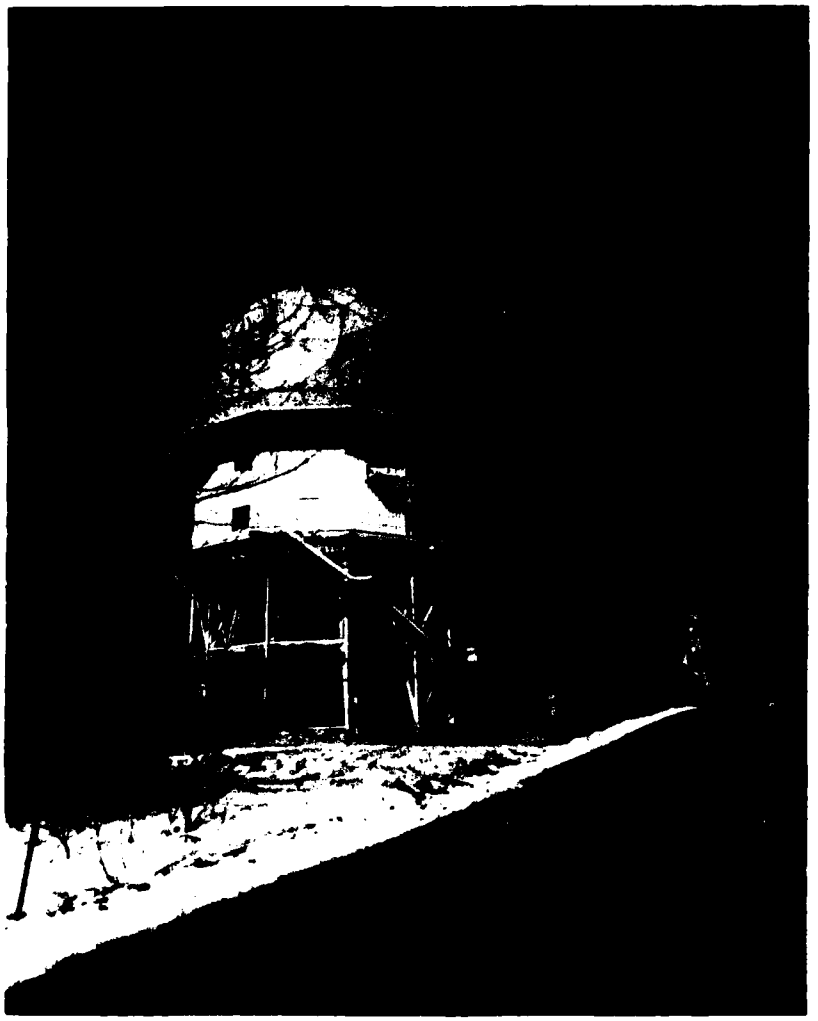

Figure 24. AB-563 Tower With Extension and CW-860 Radome

3.5 Station Primary Power

To provide uninterrupted power during operational periods and condition the commercial power, two EMU-17S diesel generators and a mechanical rotary regulator were installed. Each generator has an output capacity of 100 kVa and the regulator is rated at 50 kVa. Switchgear illustrated in the one-line schematic (Figure 25) is controlled by the switch panel shown in Figure 26, which allows for complete flexibility in choice of power source and voltage regulation.

4. CONCLUDING REMARKS

During the coming years, this radar is expected to serve two primary functions. In the near term, it is one of several radars which will play important roles in the examination of NEXRAD-related technologies. Evaluation of the performance of this radar will provide information on NEXRAD issues involving clutter cancellation and range-velocity ambiguity reduction as well as those concerning radar system calibration and hardware fault tolerance and/or location. Similarly, this system and its excellent on-line data processing and archiving equipments will be used as one of the principal test beds for NEXRAD-related efforts to develop and/or evaluate effective automated techniques for the detection and warning of atmospheric hazards. In the longer term, it is anticipated that the radar will serve as an integral part of AFGL's ground-based remote sensing research and development activities for many years. It will soon become a link in a joint AFGL-MIT Department of Meteorology dual Doppler investigation of New England winter storms, and in the succeeding years, the dual frequency Doppler system's capabilities will be supplemented with the addition of both pulse-to-pulse linear and circular polarization diversity capabilities for the investigation of precipitation processes.

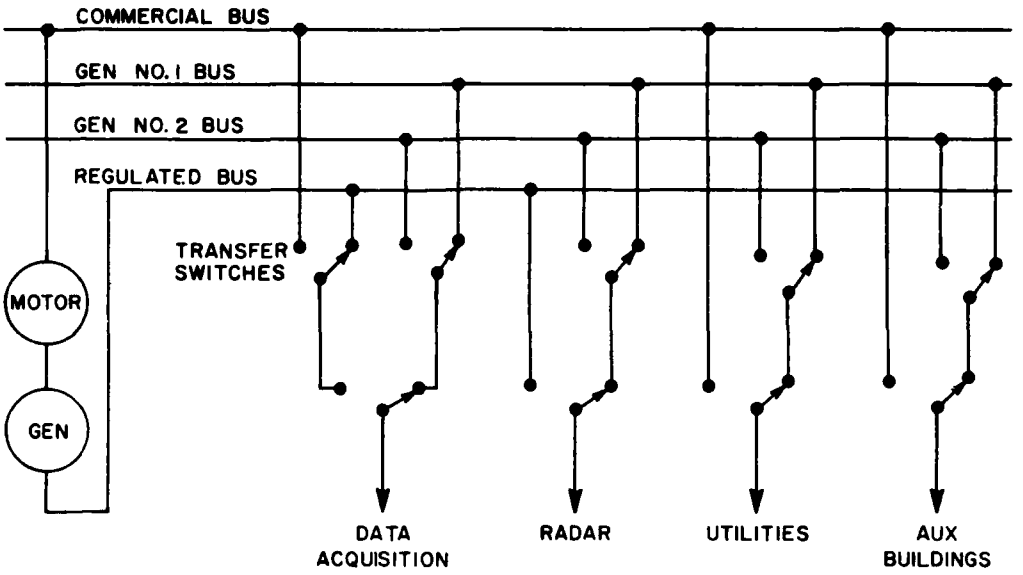

Figure 25. Station Primary Power Distribution (One-Line Drawing)

Figure 26. Switchgear Master Control Panel

References

1. Doviak, R.J., Sirmans, D.S., Zrnic', D.S., and Walker, G.B. (1978) Considerations for pulse Doppler radar observations of severe thunderstorms, J. Appl. Meteorol. 17:189-205.

2. Doviak, R.J., Zrnic', D.S., and Sirmans, D.S. (1979) Doppler weather radar, Proc. IEEE 67:1522-1533.

3. JDOP Staff (1979) Final Report on the Joint Doppler Operational Project (JDOP) 1976-1978. NOAA Tech. Memo, ERL NSSL-86.

4. Groginsky, H.L., and Glover, K.M. (1980) Weather radar canceller design, Preprints, 19th Conference on Radar Meteor., Am. Meteor. Soc., Boston, Mass.

5. Hamidi, S., and Zrnic', D.S. (1981) Considerations for the design of ground clutter cancellers for weather radars. Preprints, 20th Conference on Radar Meteor., Am. Meteor. Soc., Boston, Mass.

6. Novick, L.R., and Glover, K.M. (1974) Spectral mean and variance estimation via pulse pair processing. Preprints, 16th Conference on Radar Meteor., Am. Meteor. Soc., Boston, Mass.

7. Jagodnik, A.J. Jr., Young, M.J., Banis, K.J., and Glover, K.M. (1980) A programmable fault-tolerant meteorological radar signal processor, Vol. 8, 1980 Digest of Papers, Gov't Microcircuit Appl. Conf., Naval Electronic Sys. Command, Washington, D.C.

8. Glover, K.M. (1980) On the automation of weather radar information for air and ground operations. Preprints, 19th Conference on Radar Meteor., Am. Meteor. Soc., Boston, Mass.

9. Taylor, J.E., and Mattern, J. (1970) Radar Handbook, McGraw Hill, New York, Chapter 5, pp 15-16.

10. Teeter, W.L., and Bushore, K.R. (1955) A Dual-Frequency Microwave R.F. Head, U.S. Navy Electronics Lab Report No. 556.

11. Glover, K.M., Branche, J.R., Turner, J.H., and Groginsky, H.L. (1976) Precise calibration of coherent and non-coherent weather radars by means of a radar transponder. Preprint, 17th Conf. on Radar Meteor., Am. Meteor. Soc., Boston, Mass.

12. Callahan, M.A. (1980) Technical manual TM79-29, Electronic Space Systems Corp.

END

FILMED

4-83

DTIC